This paper is published as part of a *Dalton Transactions* themed issue entitled:

New Talent: Americas

Guest Editors: John Arnold, Dan Mindiola, Theo Agapie, Jennifer Love and Mircea Dincă

Published in issue 26, 2012 of *Dalton Transactions*

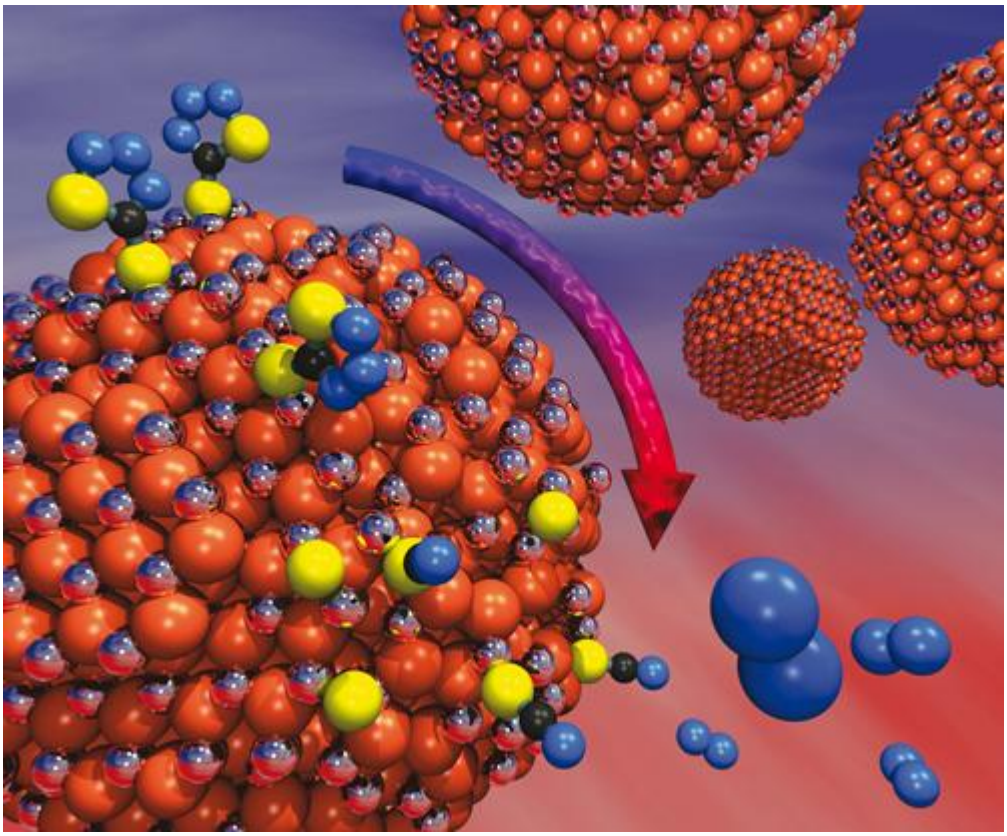

Image reproduced with permission of Richard L. Brutchey

Articles published in this issue include:

Visit the *Dalton Transactions* website for more cutting-edge inorganic chemistry
www.rsc.org/dalton

Dalton Transactions

Cite this: *Dalton Trans.*, 2012, **41**, 7969

www.rsc.org/dalton

PAPER

A redox series of gallium(III) complexes: ligand-based two-electron oxidation affords a gallium–thiolate complex†

Kristin Kowolik, Maheswaran Shanmugam, Thomas W. Myers, Chelsea D. Cates and Louise A. Berben*

Received 16th January 2012, Accepted 22nd February 2012
DOI: 10.1039/c2dt30112a

We have prepared a series of gallium(III) complexes of the redox active iminopyridine ligand (IP). Reaction of $GaCl_3$ with iminopyridine ligand (IP) in the presence of either two or four equivalents of sodium metal resulted in the formation of deep green $(IP^-)_2GaCl$ (**1**), or deep purple $[(DME)_3Na][(IP^{2-})_2Ga]$ (**2a**), respectively. Complex **1** is paramagnetic with a room temperature magnetic moment of 2.3 μ_B which falls to 0.5 μ_B at 5 K. These observations indicate that two ligand radicals comprise a triplet at room temperature which becomes a singlet due to antiferromagnetic coupling at low temperature. Complex **2** is diamagnetic. Cyclic voltammograms recorded on 0.3 M Bu_4NPF_6 THF solutions of $[Na(THF)_6][(IP^{2-})_2Ga]^-$ (**2b**) indicate that oxidation of **2b** occurs in two two-electron steps at −1.31 V and −0.54 V *vs.* SCE. The observation of two-electron redox events indicates that electronic coupling through the gallium(III) center is minimal and that the two IP ligand on **2b** are oxidized concurrently. Oxidation of **2** with one equivalent of MeS–SMe afforded the two-electron oxidized product $(IP^-)_2Ga(SMe)$ (**3**). This complex has an electronic structure analogous to **1**. Accordingly, both **1** and **3** are deep green in color and magnetic susceptibility measurements performed on **3** confirm the triplet character of the complex at room temperature. Electron paramagnetic resonance experiments on **1** and **3** display a quartet signal at $g = 2.0$ which confirmed the triplet nature of the compounds, and a half field signal consistent with the integer spin state.

Introduction

The use of redox active ligands with main group elements could give chemists the ability to explore aspects of redox chemistry usually reserved for transition metals. The limited accessibility of multiple oxidation states for the group 13 elements makes them particularly good candidates for stabilization of ligands with tuneable redox properties. Many of the known synthetic and structural reports of potentially redox-active gallium(III) complexes focus on *N*-donor ligand sets. A handful of redox-active *O*- and *S*-donor ligands sets have also been explored but are not discussed here.[1,2] Some of the earliest work on redox-active gallium(III) complexes was presented by Kaim and others and focused on the isolation of related dialkyl Ga(III) complexes of pyrazine radical anions.[3] Shortly thereafter Barron and co-workers synthesized gallium, aluminum and indium complexes containing the tridentate chelating ligand 1,3-diphenyltriazene (Hdpt).[4] See Chart 1 for depictions of ligands mentioned in the text.

Another example of a redox-active *N*-donor ligand set with gallium(III) is the first example of a homoleptic main group 1,4-di-*tert*-butyl-1,4-diazabutadiene (dbdab) complex which was reported by Cloke and coworkers.[5] Subsequent electronic structural investigations, including X-ray crystallographic and ESR measurements by Kaim, Cloke, and Green, elucidated that this complex is best formulated as gallium(III) with a mixed-valent ligand designation: $(dbdab^-)(dbdab^{2-})Ga$.[6,7] The high level of interest in the dbdab ligand stems in part from a desire to obtain an aromatic analogue of imidazolyl carbene molecules. The use of $LiGaH_4$ in the presence of dbdab and catalytic amounts of Ga metal afforded a novel hydrometallation product characterized by Smith as $[\{H_2Ga\}_2\{\mu\text{-}N(Bu^t)CH_2\}_2]$.[8] Further redox chemistry of the dbdab ligand system was reported by Cowley and co-workers who isolated compounds such as $(dbdab^{2-})Ga(\mu^2\text{-}PhCH_2NMe_2)$, a digallane $[(dbdab^{2-})Ga]_2$,[9] and the neutral

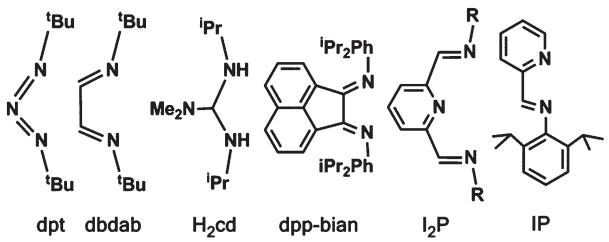

Chart 1 Ligands mentioned in the text along with their abbreviations.

Department of Chemistry, University of California, Davis, CA 95616, USA. E-mail: laberben@ucdavis.edu; Tel: +1 530-752-8475

†Electronic supplementary information (ESI) available: IR and UV-Vis spectra. CCDC reference numbers 861507–861509. For ESI and crystallographic data in CIF or other electronic format see DOI: 10.1039/c2dt30112a

ligand $[(dbdab)GaCl_2]^+$.[10] Other researchers have also employed the dbdab ligand in gallium chemistry including Schmidbaur and coworkers who used dbdab ligands to stabilize lower-valent gallium(I) molecules such as $[(dbdab^{2-})_2Ga]^-$ which was formed by potassium metal reduction of $[(dbdab^{2-})Ga]_2$. Elemental analysis and MALDI-TOF MS were used for characterization of $[(dbdab^{2-})_2Ga]^-$ rather than X-ray diffraction analysis, previously the method employed to characterized gallium complexes of dbdab.[11] Further work in this area, by Stammler and coworkers subsequently led to isolation of another monomeric gallium-containing dbdab-based heterocycle, this time stabilized by pentamethylcyclopentadienyl, $(dbdab^{2-})GaCp^*$.[12]

Some of the most recent work on redox active complexes of gallium(III) also focuses on nitrogen donor ligand sets. Bis and tris(carbodiimide) (cd) complexes of gallium(III) were synthesized by insertion of ^{i}PrNCN^{i}Pr into the Ga–N bonds of $[Ga(NMe_2)_3]_2$.[13] With the dpp-bian ligand platform (dpp-bian = 1,2-bis[(2,6-diisopropylphenyl)imino]acenaphthene), gallium(III) complexes have been obtained in a range of oxidation states,[14] and in subsequent work it was shown that the digallane $[(dpp\text{-}bian^{2-})Ga]_2$ complex adds to alkynes in a reversible fashion without breaking the Ga–Ga bond.[15] Bis(imino)pyridine complexes of gallium(III) have also been investigated. Synthesis of $(I_2P)GaI_2$ resulted from the diproportionation of "GaI" with I_2P along with formation of Ga(0).[16] In addition, we have recently shown that tetrahedral redox active gallium(III) complexes can be synthesized using bulky iminopyridine ligands (IP) with mesityl groups incorporated into the backbone.[17]

In the current work we address the synthesis of iminopyridine-based gallium(III) complexes. Moreover, we have extended these structural studies to probe redox routes to gallium–ligand bond formation following a two-electron oxidation pathway.

Experimental

Physical measurements

Elemental analyses were performed by Columbia Analytical. ^{1}H NMR spectra were recorded at ambient temperature using a Varian 400 MHz spectrometer. Chemical shifts were referenced to residual solvent. Electrochemical measurements were recorded in a glovebox under a dinitrogen atmosphere using a CH Instruments Electrochemical Analyzer, a glassy carbon working electrode, a platinum wire auxiliary-electrode, and an $Ag/AgNO_3$ nonaqueous reference electrode. Reported potentials are all referenced to the SCE couple, and were determined using decamethylferrocene as an internal standard. The number of electrons passed in a given redox process was estimated by comparison of the peak current with the peak current of decamethylferrocene included as an internal standard. UV-Vis-NIR spectra were recorded in THF solutions using a Lambda 750 UV-Vis-NIR spectrophotometer. Magnetic measurements were recorded using a Quantum Designs MPMS XL magnetometer at 0.1 T. The sample was contained under nitrogen in a gelcap and suspended in the magnetometer in a plastic straw. The magnetic susceptibility was adjusted for diamagnetic contributions using the constitutive corrections of Pascal's constants. EPR measurements were performed on 100 μL dilute solutions of the compound loaded into 4 mm OD quartz tubes in the glovebox and then freeze-pump-thawed and flame-sealed on a Schlenk line. X-Band continuous-wave EPR measurements were performed at the CalEPR center at UC Davis, with a Bruker ECS106 X-band spectrometer equipped with a Bruker SHQ resonator, an EIP 548A frequency counter, and an Oxford liquid-helium cryostat. The magnetic field was calibrated with a Bruker ER036TM teslameter.

X-Ray structure determinations

X-Ray diffraction studies were carried out on a Bruker SMART 1000, a Bruker SMART APEXII, and a Bruker SMART APEX Duo diffractometer equipped with a CCD detector.[18a] Measurements were carried out at −175 °C using Mo-Kα (λ = 0.71073 Å) and Cu-Kα (λ = 1.5418 Å) radiation. Crystals were mounted on a glass capillary or Kaptan loop with Paratone-N oil. Initial lattice parameters were obtained from a least-squares analysis of more than 100 centered reflections; these parameters were later refined against all data. Data were integrated and corrected for Lorentz polarization effects using SAINT[18b] and were corrected for absorption effects using SADABS2.3.[18c]

Space group assignments were based upon systematic absences, *E* statistics, and successful refinement of the structures. Structures were solved by direct methods with the aid of successive difference Fourier maps and were refined against all data using the SHELXTL 5.0 software package.[18d] Thermal parameters for all non-hydrogen atoms were refined anisotropically. Hydrogen atoms, where added, were assigned to ideal positions and refined using a riding model with an isotropic thermal parameter 1.2 times that of the attached carbon atom (1.5 times for methyl hydrogens).

Preparation of compounds

All manipulations were carried out using standard Schlenk or glove-box techniques under a dinitrogen atmosphere. Unless otherwise noted, solvents were deoxygenated and dried by thorough sparging with Ar gas followed by passage through an activated alumina column. Deuterated solvents were purchased from Cambridge Isotopes Laboratories, Inc. and were degassed and stored over activated 3 Å molecular sieves prior to use. The iminopyridine ligand (henceforth denoted IP) was prepared according to a previously reported procedure.[19] All other reagents were purchased from commercial vendors and used without further purification.

$(IP^-)_2GaCl$ (1)

Solid sodium (0.046 g, 2.0 mmol) was added to a stirred solution of IP (0.53 g, 2.0 mmol) in ether (15 mL) and stirred for 48 h. Solid $GaCl_3$ (0.18 g, 1.0 mmol) was slowly added to the dark red solution. The resulting green solution was allowed to stir for 24 h during which time a solid white precipitate formed. The mixture was filtered through celite to remove salts. The volume of solution was reduced to 10 mL and cooled to −25 °C overnight during which time **1** precipitated as a green powder (0.47 g, 74%). Crystals suitable for X-ray diffraction were obtained by cooling a concentrated hexane solution at −25 °C

for 3 days. IR (KBr): 1586 (m, C_{im}–N_{im}) cm^{-1}. UV-vis spectrum (THF) λ_{max} (ε_M): 245 (35 100), 360 (36 000), 418 (11 400), 453 (10 300), 662 (br, 4900) nm (L mol^{-1} cm^{-1}). Anal. calcd for $C_{36}H_{44}GaN_4Cl$: C, 67.78; H, 6.95; N, 8.78. Found: C, 67.92; H, 7.06; N, 8.69.

$[(DME)_3Na][(IP^{2-})_2Ga]$ (2a)

Solid sodium (1.1 g, 47 mmol) was added to a stirred solution of IP (5.0 g, 19 mmol) in DME (30 mL) and stirred for two hours. Solid $GaCl_3$ (1.66 g, 9.4 mmol) was carefully added to the dark red solution which was stirred for 24 h during which time a white precipitate formed. The solution was evaporated to dryness and extracted into ether (200 mL). The dark purple mixture was filtered through celite to remove salts. The solution was concentrated to 50 mL and cooled to −25 °C overnight, to afford **2a** as a purple powder (7.3 g, 89%). ^{1}H NMR (400 MHz, C_6D_6): δ 7.22 (dd, J = 2.78, 6.25, 4H, Ph), 7.08 (m, 2H, Ph), 6.75 (d, J = 6.27, 2H, py), 5.86 (d, J = 9.33, 2H, py), 5.57 (s, 2H, imC*H*), 5.33 (dd, J = 5.47, 9.97, 2H, py), 4.57 (t, J = 5.47, 2H, py), 4.19 (hept, J = 6.75, 2H, C*H*$(CH_3)_2$), 3.32 (hept, J = 7.24, 2H, C*H*$(CH_3)_2$), 2.96 (s, DME), 1.87 (d, J = 7.18, 6H, CH$(CH_3)_3$), 1.46 (d, J = 7.18, 6H, CH$(CH_3)_3$), 1.37 (d, J = 6.56, 6H, CH$(CH_3)_3$), 0.51 (d, J = 6.56, 6H, CH$(CH_3)_2$). IR (KBr): 1567 (s, C_{im}–N_{im}) cm^{-1}. UV-vis spectrum (THF) λ_{max} (ε_M): 252 (47 400), 305 (34 200), 352 (25 500), 556 (6400) nm (L mol^{-1} cm^{-1}). Anal. Calcd for $C_{48}H_{74}GaN_4O_6Na$: C, 64.35; H, 8.33; N, 6.25. Found: C, 64.66; H, 8.46; N, 6.04.

$[Na(THF)_6][(IP^{2-})_2Ga]$ (2b)

Compound **2a** (0.892 g, 1 mmol) was stirred in 10 mL of THF and then the solution was concentrated to 2 mL and 10 mL of hexanes was layered on top. After being cooled at −25 °C overnight **2b** (0.99 g, 94%) was obtained as a dark purple solid. Crystals suitable for X-ray diffraction were grown by slow diffusion of pentane into a concentrated THF solution at −25 °C. ^{1}H NMR (400 MHz): δ 7.32 (d, J = 3.41, 2H, Ph), 7.25 (dd, J = 5.45, 8.27, 4H, Ph), 6.90 (d, J = 6.52, 2H, py), 5.98 (d, J = 9.60, 2H, py), 5.63 (s, 2H, imC*H*), 5.46 (dd, J = 4.99,9.02, 2H, py), 4.71 (t, J = 6.50, 2H, py), 4.41 (hept, J = 6.26, 2H, C*H*$(CH_3)_2$), 3.45 (hept, J = 6.15, 2H, C*H*$(CH_3)_2$), 2.79 (s, 24H, bound THF), 1.97 (d, J = 6.59, 6H, CH$(CH_3)_2$), 1.59 (d, J = 7.14, 6H, CH$(CH_3)_2$), 1.46 (d, J = 6.59, 6H, CH$(CH_3)_2$), 0.61 (d, J = 7.14, 6H, CH$(CH_3)_2$). IR (KBr): 1567 (s, C_{im}–N_{im}) cm^{-1}. UV-vis spectrum (THF) λ_{max} (ε_M): 306 (33 900), 363 (25 200), 524 (6700), 561 (6400), 610 (5400) nm (L mol^{-1} cm^{-1}). Anal. Calcd for $C_{60}H_{92}GaN_4NaO_6$: C, 68.11; H, 8.76; N, 5.29. Found: C, 68.15; H, 8.54; N, 5.46.

$[\{(Et_2O)_2NaIP^{2-}\}(IP^{2-})Ga]$ (2c)

Solid sodium (1.1 g, 47 mmol) was added to a stirred solution of IP (5.0 g, 19 mmol) in diethyl ether (30 mL). After 48 h, solid $GaCl_3$ (1.66 g, 9.4 mmol) was carefully added to the dark red solution which was then stirred for 48 h during which time a white precipitate formed. The solution was filtered through celite to remove salts and then concentrated to one third its volume. After addition of hexane the solution was cooled to −25 °C overnight, to afford **2c** as a deep purple powder (5.7 g, 78%). ^{1}H NMR (600 MHz, C_6D_6): δ 7.25 (d, J = 7.09, 2H, Ph), 7.09 (t, J = 6.42, 2H, Ph), 6.84 (d, J = 7.17, 2H, Ph), 6.46 (m, 2H, py), 6.15 (d, J = 9.55, 2H, py), 5.67 (m, 2H, py), 5.53 (s, 2H, imC*H*), 4.67 (s, 2H, py), 3.76 (hept, J = 6.73, 2H, $CH(CH_3)_2$), 3.46 (s, ether), 1.74 (s, ether), 1.15 (d, J = 5.48, 6H, $CH(CH_3)_2$), 0.66 (d, J = 5.48, 6H, $CH(CH_3)_2$) ppm. IR (KBr): 1567 (s, C_{im}–N_{im}) cm^{-1}. UV-vis spectrum (THF) λ_{max} (ε_M): 252 (47 400), 305 (34 200), 352 (25 500), 556 (6400) nm (L mol^{-1} cm^{-1}). Anal. Calcd for $C_{44}H_{64}GaN_4O_2Na$: C, 68.30; H, 8.34; N, 7.24. Found: C, 68.55; H, 8.07; N, 6.98.

$(IP^-)_2Ga(SMe)$ (3)

Compound **2c** (1.0 g, 1.29 mmol) was stirred in 10 mL of THF for about 5 min giving a deep purple solution. Dimethyl disulfide (0.115 mL, 1.29 mmol) was carefully added *via* syringe under nitrogen stream resulting in a quick color change from deep purple to dark green. The mixture was evaporated to dryness and after addition of hexane was filtered through celite. The solution was allowed to dry under vacuum for about 10 h. A green powder of **3** was collected (0.354 g, 40%) and crystals suitable for X-ray diffraction were grown by slow diffusion of pentane into a concentrated THF solution at −25 °C. IR (KBr): 1586 (m, C_{im}–N_{im}) cm^{-1}. UV-vis spectrum (THF) λ_{max} (ε_M): 236 (51 280), 359 (19 784), 414 (4549), 441 (3847), 665 (br, 466) nm (L mol^{-1} cm^{-1}). Anal. Calcd for $C_{36}H_{44}GaN_4S$: C, 68.41; H, 7.29; N, 8.63. Found: C, 68.73; H, 7.03; N, 8.56.

Results and discussion

Synthesis and characterisation of $(IP^-)_2GaCl$ (1)

Synthesis of a two-electron reduced Ga(III) complex was achieved following methods similar to those we have used to access analogous Al(III) complexes (Scheme 1).[20] Reaction of two equivalents of sodium metal and two equivalents of IP with $GaCl_3$ in ether gave, upon workup, $(IP^-)_2GaCl$ (**1**) as a deep green solid. Complex **1** is soluble in ether, alkane, and aromatic solvents but due to its paramagnetic nature, NMR spectra are

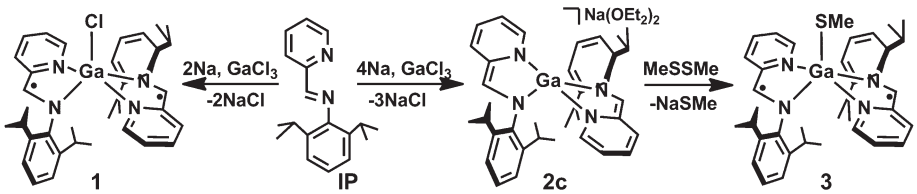

Scheme 1 Synthesis of compounds **1**–**3**.

Table 1 Crystallographic data[a] for the complexes $(IP^{-})_2GaCl$ (**1**), $[(THF)_6Na][(IP^{2-})_2Ga]$ (**2b**), and $(IP^{-})_2Ga(SMe)$ (**3**)

	1	**2b**	**3**
Formula	$C_{36}H_{44}ClGaN_4$	$C_{64}H_{98}GaN_4NaO_6$	$C_{41}H_{55}GaN_4OS$
Crystal size	0.18 × 0.13 × 0.09	0.27 × 0.21 × 0.13	0.25 × 0.19 × 0.17
FW/g mol^{-1}	637.92	1114.66	721.67
Space group	*C*2/*c*	$P2_1/c$	$P2_1/c$
a/Å	21.5436(5)	17.755(2)	11.700(1)
b/Å	9.8702(2)	15.578(2)	18.994(2)
c/Å	17.0142(4)	23.043(2)	19.129(1)
α/°	90	90	90
β/°	113.8440(10)	102.565(6)	113.022(3)
γ/°	90	90	90
V/Å^3	3309.1(1)	6220.9(9)	3882.6(6)
Z	4	4	4
T/K	90(2)	90(2)	90(2)
ρ, calcd/g cm^{-3}	1.280	1.190	1.235
Refl. coll./$2\theta_{max}$	9798/136.82	42 448/129.94	37 672/51.58
Un. ref./$I > 2\sigma(I)$	2884/2881	11 498/9947	7432/5281
No. param/restr.	191/0	717/0	442/0
λ/Å; *μ*(Kα)/cm^{-1}	1.54178	1.54178	0.71073
R_1[b]/GOF	0.0307/1.464	0.0518/1.022	0.0508/1.025
wR_2 ($I > 2\sigma(I)$)[b]	0.1489	0.1461	0.1296
Res. dens./e Å^{-3}	0.486/−0.561	0.810/−0.514	0.698/−0.537

[a] Obtained with graphite-monochromated Mo-Kα (λ = 0.71073 Å) radiation. [b] $R_1 = \Sigma||F_o| - |F_c||/\Sigma|F_o|$, w$R_2 = \{\Sigma[w(F_o^2 - F_c^2)^2]/\Sigma[w(F_o^2)^2]\}^{1/2}$.

Table 2 Selected average interatomic distances (Å) and selected average angles (°) for complexes with one-electron reduced IP ligands in $(IP^{-})_2GaCl$ (**1**) and $(IP^{-})_2Ga(SMe)$ (**3**) (this work), $(IP^{-})_2AlCl$ (prior work)[20]

	$(IP^{-})_2AlCl$	**1**	**3**
M–N_{im}	1.915(1)	1.955(1)	1.964(3)
M–N_{py}	2.009(15)	2.079(1)	2.110(3)
M–X[a]	2.191(1)	2.228(1)	2.251(1)
C_{im}–N_{im}	1.354(2)	1.353(2)	1.354(4)
C_{im}–C_{py}	1.405(2)	1.402(2)	1.402(5)
C_{py}–N_{py}	1.366(2)	1.368(2)	1.370(3)
N_{im}–M–N_{py}	81.46(6)	80.73(5)	79.8(1)
N_{py}–M–$N_{im'}$	93.85(6)	95.36(5)	93.8(1)
N_{im}–M–$N_{im'}$	125.28(6)	126.22(7)	124.0(1)
N_{py}–M–$N_{py'}$	169.59(6)	171.42(7)	166.4(1)
X–M–N_{im}	117.87(5)	116.89(3)	117.91(9)
X–M–N_{py}	95.21(5)	94.29(4)	96.81(9)
C_{py}–C_{im}–N_{im}	116.73(14)	118.4(1)	118.3(3)
τ	0.739	0.753	0.706

[a] X = Cl, O, S; R = H, Me.

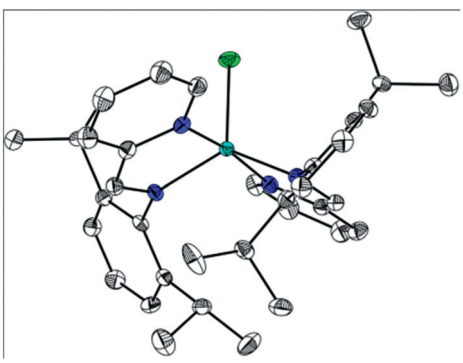

Fig. 1 Solid state structure of $(IP^{-})_2GaCl$ in **1**. Light blue, white, blue, and red, ellipsoids represent Ga, C, N, and O atoms, respectively. Ellipsoids at 50%, H atoms are omitted.

uninformative. The most distinctive features of the UV-visible absorption spectrum are a sharp band at 360 (ε = 36 000) and a broad band at 662 nm (4900 L mol^{-1} cm^{-1}), consistent with the deep green color of the complex (Fig. S1†).

The solid state structure of **1** was investigated on a single crystal grown by chilling a concentrated hexanes solution of the complex to −25 °C for about one week (Tables 1, 2, and Fig. 1). In compound **1** the gallium center is approximately trigonal bipyramidal and bond distances and angles are in accord with previous reports of the IP ligand in the 1$^-$ oxidation state (Table 2).[21,20] The C–N bond of the imine functional group falls between the length of a typical C–N single and double bond at 1.353(2) Å. The Ga–N_{im} and Ga–N_{py} bond lengths are slightly longer than those in the analogous aluminum complex (Table 2), at 1.955(1) and 2.079(1) Å, respectively, and are consistent with the Ga–N bond lengths we have previously observed when using the bulkier mesityl-substituted IP ligand in the 1$^-$ oxidation state.[17] Furthermore, other trends such as chelate ligand bite angle at 80.73(5)° are consistent with the 1$^-$ oxidation state of IP. Based on the value of τ = 0.753, the overall geometry of the complex can be most accurately described as trigonal bipyramidal and this is very similar to the analogous aluminum complex which had a value for τ of 0.739.[22]

Electrochemical measurements were performed on **1** in 0.3 M Bu_4NPF_6 THF solutions using a glassy carbon working electrode (Fig. 2 and Table S1†). A reversible two-electron reduction wave was observed at −1.57 V *vs.* SCE and two-electron oxidation of **1** occurred in two, successive one-electron steps at −0.62 V and −0.19 V *vs.* SCE. The spacing between these two oxidation couples corresponds to a comproportionation constant of $K_c = 4.7 \times 10^7$ for the reaction $\mathbf{1}^{2+} + \mathbf{1} \leftrightarrow 2\ \mathbf{1}^{+}$. Compound **1** possesses a K_c value 1.5 orders of magnitude larger than

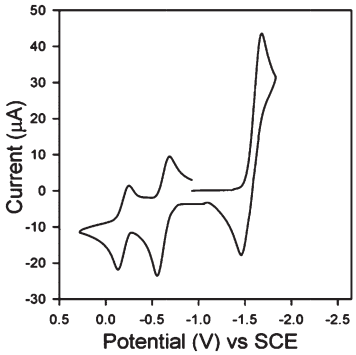

Fig. 2 CV of **1** recorded in 0.3 M Bu_4NPF_6 THF solution. Glassy carbon working electrode.

$(IP^-)_2AlCl$ which was $10^{5.8}$. We do not yet know whether this is due to better electronic communication mediated by the more diffuse orbitals of gallium *vs.* aluminum.

Synthesis and characterisation of $[(IP^{2-})_2Ga]^-$ (2)

Syntheses of four-electron reduced Ga(III) complexes were achieved using 4.5 equivalents of sodium metal added to a DME reaction solution of $GaCl_3$ and two equivalents of IP. $[Na(DME)_3][(IP^{2-})_2Ga]$ (**2a**) was obtained as a deep purple solid from DME, and $[Na(THF)_6][(IP^{2-})_2Ga]$ (**2b**) could be obtained after stirring **2a** in a THF solution overnight. $[\{(OEt_2)_2NaIP^{2-}\}-[(IP^{2-})Ga]^-$ (**2c**) was obtained when the reaction was performed in diethyl ether.

The four electron reduced complexes **2a**, **2b**, and **2c** are diamagnetic and ^{1}H-NMR spectroscopy measurements definitively identify the compounds. As an example, resonances for the protons on the dearomatized pyridine rings were observed between 6.75 and 4.57 ppm for **2a** and the imine CH resonance was observed as a singlet at 5.57 ppm. Other solution properties of complexes **2a–2c** also bear resemblance to the solution properties of $[Na(DME)_3][(IP^{2-})_2Al]$.[20] For example, UV-visible absorption spectra of **2a** displays intense bands at 352 (34 200) and 556 (6400) nm (L mol^{-1} cm^{-1}) which are representative of the deep purple color observed in each of the complexes **2a–2b**.

To probe the structural properties of four electron reduced gallium(III) complexes, the solid state structure of **2b** was investigated. Single crystals were grown by chilling a concentrated THF solution of the complex to −25 °C for about one week (Tables S1,† 3, and Fig. 3). Complex **2b** is tetrahedral and the bond distances and angles in that complex are consistent with the IP^{2-} oxidation state of the ligand.[20,21] The bond distances for C_{im}–C_{py}, C_{im}–N_{im} and C_{im}–N_{py} in **2b** are 1.365(3), 1.405(3) and 1.376(3) Å, respectively. The average bond distances observed for the doubly reduced Al complex were 1.356(6), 1.414(6) and 1.399(6) Å, respectively (Table 3).

Electrochemical measurements were performed on **2b** in 0.3 M Bu_4NPF_6 THF solutions using a glassy carbon working electrode (Fig. 3, top right). Two reversible two-electron oxidation events were observed at −1.31 V and −0.54 V *vs.* SCE. The observation of two-electron, rather than one-electron redox events indicates that electronic coupling through the gallium(III) center is minimal and that the two IP ligands on **2b** are oxidized

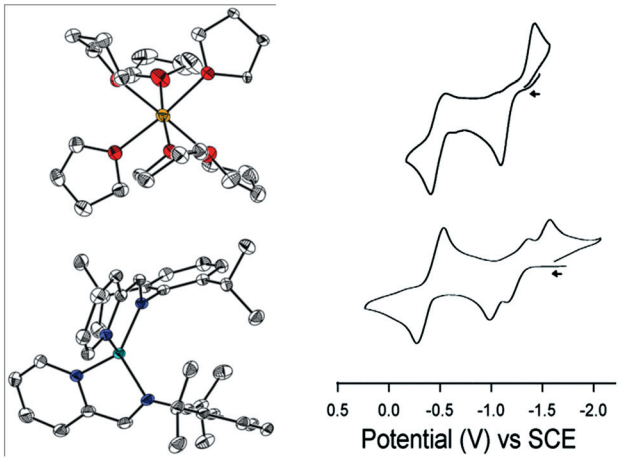

Fig. 3 (left) Solid state structure of $[Na(THF)_6][(IP^{2-})_2Ga]$ **2b**. Light blue, white, blue, red, and orange ellipsoids represent Ga, C, N, O, and Na atoms, respectively. Ellipsoids at 50%, H atoms are omitted. (right) CVs of **2b** (top), and of $[Na(DME)_3][(IP^{2-})_2Al]$ (bottom)[20] recorded in 0.3 M Bu_4NPF_6 THF solution using a glassy carbon working electrode.

Table 3 Selected average interatomic distances (Å) and selected average angles (°) for the group 13 metal complex in $[Na(DME)_3][(IP^{2-})_2Al]$ (prior work),[20] and in $[Na(THF)_6][(IP^{2-})_2Ga]$ (**2b**) (this work)

	$[(IP^{2-})_2Al]^-$	**2b**
M–N_{im}	1.844(4)	1.907(2)
M–N_{py}	1.873(4)	1.917(2)
C_{im}–N_{im}	1.414(6)	1.405(3)
C_{im}–C_{py}	1.356(6)	1.365(3)
C_{py}–N_{py}	1.399(6)	1.376(3)
N_{im}–M–N_{py}	87.87(2)	86.60(8)
N_{py}–M–$N_{im'}$	125.87(2)	126.75(8)
N_{im}–M–$N_{im'}$	123.55(12)	119.88(9)
N_{py}–M–$N_{py'}$	112.50(2)	114.77(9)
C_{py}–C_{im}–N_{im}	117.1(4)	117.6(2)

concurrently. This result is in contrast to our observations for the analogous aluminum complex $[Na(DME)_3][(IP^{2-})_2Al]$ (Fig. 3, bottom right). We reported previously that the first two oxidation events for $[Na(DME)_3][(IP^{2-})_2Al]$, that is for oxidation to the IP^- state of both ligands occurred at −1.36 V and −1.17 V, respectively. We currently have no explanation for the observed differences. Structural examinations have revealed that the geometry of the two complexes are very similar (Table 2).

Two-electron oxidation of 2c to $(IP^{2-})_2Ga(SMe)$ (3)

We have previously found that two-electron oxidation reactions and aluminum–oxygen bond formation can be achieved by reaction of $[Bu_4N][(IP^{2-})_2Al]$ with pyridine-*N*-oxide and this reaction afforded $(IP^-)_2Al(OH)$.[23] In an effort to develop an alternate route to gallium(III) complexes of the form $(IP^-)_2GaX$ (where X = O, S, or N) and to illustrate that redox reactivity can be accessed *via* ligand-based events, we have explored the reaction of **2c** with peroxide analogue, MeSSMe.

Accordingly, reaction of **2c** with one equivalent of MeS–SMe was stirred at room temperature for 30 min during which time the deep purple color of **2c** was replaced by a deep green color.

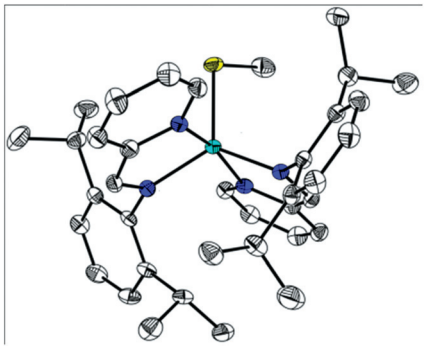

Fig. 4 Solid state structure of $(IP^{-})_2Ga(SMe)$ in **3**. Light blue, white, blue, and yellow ellipsoids represent Ga, C, N, and S atoms, respectively. Ellipsoids are shown at 50%, H atoms are omitted.

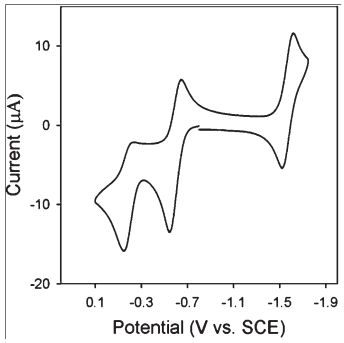

Fig. 5 CV of **3** recorded in 0.3 M Bu_4NPF_6 THF solution. Glassy carbon working electrode.

This color is typical of the singly reduced ligands in $(IP^{-})_2MX$ complexes which we have previously observed (M = Al, Ga; X = Cl, OH, CF_3SO_3). The reaction afforded $(IP^{-})_2Ga(SMe)$ (**3**) (Scheme 1). In this reaction, a two-electron oxidation of the $[(IP^{2-})_2Ga]^{-}$ moiety has been effected by the two-electron oxidant MeS–SMe. However, only one $^{-}$SMe ligand is transferred to the gallium coordination sphere. Presumably the remaining equivalent of MeS^{-}, which is necessary to balance the reaction, is lost as MeSNa.

Complex **3** is soluble in ethers as well as aromatic solvents but is only slightly soluble in alkanes. NMR data is uninformative due to the paramagnetic nature of **3**. The UV-visible absorption spectrum shows a peak at 359 nm (ε = 19784) and a peak at 665 nm (ε = 466) which are in agreement with the spectrum for complex **1**. The IR spectrum of **3** displayed an absorption band at 1586 cm^{-1} (Table S2 and Fig. S2†) which is consistent with the C–N_{im} functional group of an IP ligand in the 1^{-} oxidation state.[24]

Single crystals of **3** suitable for X-ray diffraction analysis were obtained in 40% yield by diffusion of pentane into a THF solution of the product (Tables 1, 2, S1†, and Fig. 4). The solid state structure confirmed the assignment of **3** as the biradical complex $(IP^{-})_2Ga(SMe)$ (**3**). The bond lengths and angles of **3** agree with the IP^{-} oxidation state assigned by IR spectroscopy. For example, the C–N_{im} bond of **3** is equal within error to the bond length of the previously reported $(IP^{-})_2AlCl$ complex (Table 2), and the Ga–N_{im} and Ga–N_{py} bond lengths for **3** are 1.964(3) Å and 2.110(3) Å. The distances are 0.05 and 0.10 Å longer than the corresponding bond lengths in $(IP^{-})_2AlCl$, consistent with the larger ionic radius of Ga^{3+} compared with Al^{3+}. The Ga–S bond length is 2.251(1) Å and is consistent within error with reported literature values for Ga–S bonds.[14,26] The N_{im}–Ga–N_{py} bond angle is 79.8° and is in agreement with bite angles reported for IP^{-} including previous results reported for both aluminum and gallium complexes.[17,20] The N_{py}–Ga–N_{py} bond angle for **3** (166.4(1)°) is notably smaller than for **1** (171.42(7)°). The N–Ga–N angle difference between compound **1** and **3** could be due to electronics (Cl *vs.* S as a coordinating atom) or simply sterics, the SMe group is oriented such that it is impinging upon the volume of one of the pyridine moieties in **3**. In addition, the gallium center in **3** has τ = 0.706 which is a little smaller than τ values for any other of the five-coordinate complexes that we have reported for IP.[20] For example, **1** had τ = 0.753, and $(IP^{-})_2AlCl$ has τ = 0.739. However, τ = 0.706 is still consistent with a trigonal bipyramidal geometry.[22]

Electrochemical measurements were performed by cyclic voltammetry experiments with 0.3 M Bu_4NPF_6 THF solutions of **3** and using a glassy carbon working electrode (Fig. 5, and Table S1†). A reversible two-electron reduction wave was observed at −1.52 V *vs.* SCE. In contrast to our previous reports for complexes of the form $(IP^{-})_2MX$ (where M = Al, Ga; X = Cl, OH, CF_3SO_3) there is little evidence for the presence of irreversible ligand-based reduction events for complex **3**. Two-electron oxidation of **3** occurred in two successive steps at −0.54 V and −0.16 V *vs.* SCE.

One other example of redox chemistry being exploited to yield Ga–S bonds was reported by Fedushkin and co-workers. Notably, in this previous case, redox chemistry is metal rather than ligand-centered and formation of a monomeric gallium dithiolate complex resulted from reaction of the digallane complex $[(dpp\text{-}bian^{2-})Ga]_2$ with various disulfides. Disubstituted complexes such as $[(dpp\text{-}bian^{2-})Ga(S_2CNMe_2)_2$ were obtained.[14] We know of no other example where *ligand-based* redox chemistry facilitates metal substitution for a gallium(III) complex. Heyduk and coworkers have demonstrated similar ligand-based reactivity with zirconium complexes, and Abu-Omar and coworkers reported O_2 activation *via* a ligand-based redox process.[25]

There are a limited number of monomeric gallium–thiolate complexes, and all of them were obtained by metathesis, rather than redox chemistry routes. Examples of these various complexes include a report by Long and coworkers of $GaCl_2(4\text{-}Mepy)_2(\mu^2\text{-}S_2CNEt_2)$ derived from gallium(II) chloride "Ga[$GaCl_4$]" and tetraethylthiuram disulfide in 4-methylpyridine.[26] Moreover, the thiolates 2-mercaptopyridine and 2-diethylaminoethanethiol·HCl have been employed to access compounds such as $(\mu^2\text{-}Spy)_2GaMe$ and $AlH(SCH_2CH_2NEt_2)_2$, respectively.[27,28] Each of the above-mentioned reactions are notable in that they yield monomeric, rather than oligomeric Ga–S containing products. Dimeric Ga–S containing products are also noteworthy, and include $[\{HC(MeCDippN)_2\}GaS]_2$ formed from elemental sulfur (where HC(MeCDippN is a bulky β-diketimidate ligand).[29]

Electronic structures

The electronic structures of each of the two-electron reduced complexes, **1** and **3**, were probed using SQUID-detected

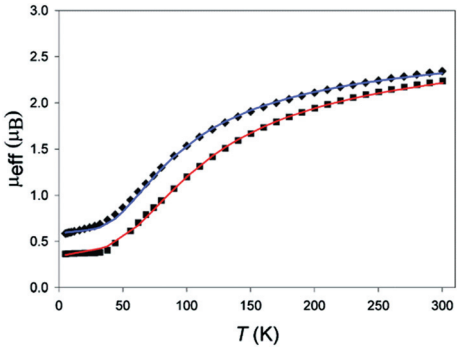

Fig. 6 Magnetic susceptibility measurements performed on **1** and **3** at 1000 Oe between 5–300 K. Triangles and circles represent the experimental data for **1** and **3**, respectively, and blue and red solid lines represent fits to the data for **1** and **3**, respectively, using a spin Hamiltonian of the form $\hat{H} = -2J\hat{S}_{L(1)} \cdot \hat{S}_{L(2)}$. Fit parameters: **1**, g = 2.0, J = −100 cm^{-1}, TIP = 0.2 × 10^{-3} emu, paramagnetic impurity = 1%; **3**, g = 2.0, J = −79 cm^{-1}, TIP = 0.2 × 10^{-3} emu, paramagnetic impurity = 3.2%.

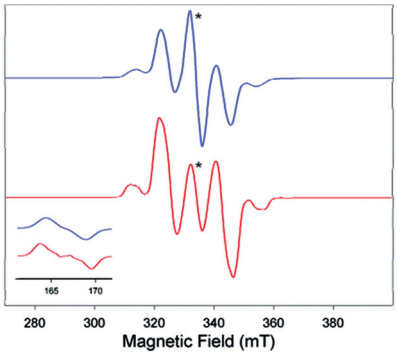

Fig. 7 X-Band cw EPR spectrum of a frozen solution of 2 mM **1** (red) and **3** (blue) in frozen toluene. Experimental parameters: microwave frequency 9.389 GHz, power 20 mW, temperature 100 K, modulation amplitude 5 mT. The asterisk indicates the doublet signal.

magnetic susceptibility measurements (Fig. 6). Magnetic susceptibility measurements were performed on solid samples of **1** and **3** between 5 and 300 K in an applied field of 1000 Oe. For **1** the room temperature magnetic moment of 2.3 μ_B dropped to 0.5 μ_B in a similar pattern that we have previously observed for $(IP^-)_2AlCl$.[20] This data supports an electronic structure model where two ligand centered radicals result in observation of a triplet at room temperature, which becomes a singlet at 5 K as a result of antiferromagnetic coupling through aluminum. In order to probe the observed interaction quantitatively the experimental data was fit using MAGFIT3.1[30] and a spin Hamiltonian of the form $\hat{H} = -2J\hat{S}_{L(1)} \cdot \hat{S}_{L(2)}$ along with g = 2.0. The results support an electronic model in which two (IP^-)-based ligand radicals interact antiferromagnetically with an energy of J = −100 cm^{-1}. A similar electronic structure model was found for complex **3**. In this case the energy of the antiferromagnetic coupling interaction is J = 79 cm^{-1}. These moderate values for exchange coupling between iminopyridine ligands are very similar to values reported by Wieghardt and coworkers for exchange coupling mediated by the first row transition elements.[21]

To confirm the electronic structure model obtained using bulk magnetic measurements, electron paramagnetic resonance (EPR) measurements were performed on samples of **1** and **3** (Fig. 7). Measurements performed on dilute frozen toluene solutions at 100 K for each of these samples revealed a pattern consisting of four lines between 310 and 360 mT characteristic of a triplet state (S = 1) as well as a single line due to a doublet species (S = 1/2) (Fig. 7). Both signals are centered at 333 mT, g = 2.018(1), typical for carbon or nitrogen-centered delocalized organic radicals.

The triplet nature of the four-line spectrum is confirmed by the additional presence of a weak Δm_S = ±2 transition at half field (Fig. 7, inset). The amount of monoradical varies between EPR sample preparations from the same batch of solid sample and we attribute this signal to reaction of the complexes with trace amounts of dioxygen introduced during the preparation of the EPR samples and the high sensitivity of the complexes toward water and dioxygen. The pertinent features of these EPR spectra are well-aligned with those of $(IP^-)_2AlCl$ which we have previously discussed in detail.[20]

Conclusions

A redox series of gallium(III) complexes has been synthesized and an example of a ligand-based redox transformation has been demonstrated. We have shown that the electronic properties of these gallium(III) complexes are similar to the properties which we previously described for the analogous aluminum(III) complexes. In complex **1** each IP ligand is reduced by one electron and the complex exhibits a deep green color. Complexes **2a–2c** contain two IP ligands that are each reduced by two electrons and both complexes are deep purple in color. Furthermore, we have demonstrated that two-electron oxidation of tetrahedral **2c** can be mediated by MeS–SMe along with transfer of one ligand MeS^- equivalent to yield a five-coordinate gallium(III) thiolate complex (**3**) *via* a *ligand-based* redox process. Complexes **1** and **3** exhibit a triplet spin state at room temperature as a result of an unpaired electron localized at each of the IP^- ligands. These electronic structures were confirmed by observation of a four line signal in their EPR spectra. Moreover, each of the complexes **1** and **3** displays a reversible two-electron oxidation, and two-electron reduction event when probed using cyclic voltammetry measurements in THF solution. Our current work focuses on developing the oxidation chemistry described herein to provide ligand-based redox pathways to Ga–O and Ga–N bond formation and subsequent small molecule activation *via* insertion pathways.

We thank the University of California Davis for funding, and D. Robles and Prof. R. D. Britt for assistance with EPR spectroscopy measurements.

Notes and references

1 M. Lanznaster, H. P. Hratchian, M. J. Hegg, L. M. Hryhorczuk, B. R. McGarvey, H. B. Schlegel and C. N. Verani, *Inorg. Chem.*, 2006, **45**, 955.
2 C. R. Kowol, E. Reisner, I. Chiorescu, V. B. Arion, M. Galanski, D. V. Deubel and B. K. Keppler, *Inorg. Chem.*, 2008, **47**, 11032.
3 W. Kaim, *Z. Naturforsch. B: Anorg. Chem. Org. Chem.*, 1981, **36b**, 677.

4 J. T. Leman and A. R. Barron, *Polyhedron*, 1989, **8**, 1909.
5 F. G. N. Cloke, G. R. Hanson, M. J. Henderson, P. B. Hitchcock and C. L. Raston, *Chem. Commun.*, 1989, 1002.
6 W. Kaim and W. Matheis, *Chem. Commun.*, 1991, 597.
7 F. G. N. Cloke, C. I. Dalby, P. J. Daff and J. C. Green, *Chem. Commun.*, 1991, 181.
8 M. J. Henderson, C. H. L. Kennard, C. L. Raston and G. Smith, *Chem Commun.*, 1990, 1203.
9 D. S. Brown, A. Decken and A. H. Cowley, *J. Am. Chem. Soc.*, 1995, **117**, 5421.
10 J. A. C. Clyburne, R. D. Culp, S. Kamepalli, A. H. Cowley and A. Decken, *Inorg. Chem.*, 1996, **35**, 6651.
11 E. S. Schmidt, A. Jockisch and H. Schmidbaur, *J. Am. Chem. Soc.*, 1999, **121**, 9758.
12 T. Pott, P. Jutzi, B. Neumann and H. G. Stammler, *Organometallics*, 2001, **20**, 1965.
13 A. P. Kennedy, G. P. A. Yap, D. S. Richeson and S. T. Barry, *Inorg. Chem.*, 2005, **44**, 2926.
14 I. L. Fedushkin, A. S. Nikipelov, A. A. Skatova, O. V. Maslova, A. N. Lukoyanov, G. K. Fukin and A. V. Cherkasov, *Eur. J. Inorg. Chem.*, 2009, 3742.
15 I. L. Fedushkin, A. S. Nikipelov and K. A. Lyssenko, *J. Am. Chem. Soc.*, 2010, **132**, 7874.
16 T. Jurca, K. Dawson, I. Mallow, T. Burchell, G. P. A. Yap and D. S. Richeson, *Dalton Trans.*, 2010, **39**, 1266.
17 T. W. Myers and L. A. Berben, *Inorg. Chem.*, 2011, 47.
18 (*a*) SMART Software Users Guide, Version 5.1, Bruker Analytical X-Ray Systems, Inc., Madison, WI, 1999; (*b*) SAINT Software Users Guide, Version 7.0, Bruker Analytical X-Ray Systems, Inc., Madison, WI, 1999; (*c*) G. M. Sheldrick, SADABS, Version 2.03, Bruker Analytical X-Ray Systems, Inc., Madison, WI, 2000; (*d*) G. M. Sheldrick, SHELXTL Version 6.12, Bruker Analytical X-Ray Systems, Inc., Madison, WI, 1999; (*e*) *International Tables for X-Ray Crystallography*, Kluwer Academic Publishers, Dordrecht, 1992, vol. C.
19 T. V. Laine, M. Klinga and M. Leskelä, *Eur. J. Inorg. Chem.*, 1999, 959.
20 T. W. Myers, N. Kazem, S. Stoll, R. D. Britt, M. Shanmugam and L. A. Berben, *J. Am. Chem. Soc.*, 2011, **133**, 8662.
21 C. C. Lu, E. Bill, T. Weyhermüller, E. Bothe and K. Wieghardt, *J. Am. Chem. Soc.*, 2008, **130**, 3181.
22 A. W. Addison, T. N. Rao, J. J. Van Rijn and G. C. Verschoor, *J. Chem. Soc., Dalton Trans.*, 1984, 1349.
23 T. W. Myers and L. A. Berben, *J. Am. Chem. Soc.*, 2011, **133**, 11863.
24 Previously reported imine spectra: K. Kincaid, C. P. Gerlach, G. R. Giesbrecht, J. R. Hagadorn, G. R. Whitener, A. Shafir and J. Arnold, *Organometallics*, 1999, **18**, 5360.
25 (*a*) M. R. Hameline and A. H. Heyduk, *J. Am. Chem. Soc.*, 2006, **128**, 8410; (*b*) C. Stanciu, M. E. Jones, P. E. Fanwick and M. M. Abu-Omar, *J. Am. Chem. Soc.*, 2007, **129**, 12400.
26 E. M. Gordon, A. F. Hepp, S. A. Duraj, T. S. Habash, P. E. Fanwick, J. D. Schupp, W. E. Eckles and S. Long, *Inorg. Chim. Acta*, 1997, **257**, 247.
27 C. C. Landry, A. Hynes, A. R. Barron, I. Haiduc and C. Silvestru, *Polyhedron*, 1996, **15**, 391.
28 C. Jones, F. C. Lee, G. A. Koutsantonis, M. G. Gardiner and C. L. Raston, *J. Chem. Soc., Dalton Trans.*, 1996, 829.
29 N. J. Hardman and P. P. Power, *Inorg. Chem.*, 2001, **40**, 2474–2475.
30 E. A. Schmitt, Ph.D. thesis, University of Illinois Urbana-Champaign, Urbana, IL, 1995.

